Nonlinear dynamics of magnetic vortices in single-crystal and ion-damaged $NbSe_2$

J. Zhang and L. E. De Long
Department of Physics and Astronomy, University of Kentucky, Lexington, Kentucky 40506

V. Majidi
Department of Chemistry, University of Kentucky, Lexington, Kentucky 40506

R. C. Budhani*
Materials Science Division, Brookhaven National Laboratory, Upton, New York 11973
(Received 24 April 1995; revised manuscript received 18 July 1995)

Nonlinear dynamics of magnetic flux lines in superconducting $NbSe_2$ are studied using the vibrating-reed technique and a resonance-line-shape analysis. A yield point for plastic deformation of the flux-line lattice is linked to the onset of a dissipation anomaly previously associated with a flux-line lattice melting transition. The resonance (10 kHz range) of radiation-damaged samples bifurcates into patterned sidebands at high drives, with additional nonlinear response emerging above 200 kHz, which may signal the onset of chaos.

Dissipation by mobile magnetic vortices is a major limitation to the technological utilization of high-temperature superconductors, although heavy ion irradiation of single crystals has produced promising increases in their current capacity.[1] Fundamental studies of cooperative phenomena and dynamics of vortices have addressed the existence of a controversial melting transition of the flux-line (FL) lattice (FLL) (Refs. 2,3) and revealed several distinct dissipative anomalies and a ''peak effect'' (PE) (a nonmonotonic field dependence of the critical current density J_c just below the upper critical magnetic field H_{c2}) both in $NbSe_2$ and $YBa_2Cu_3O_7$ (YBCO).[4–11] It is unlikely that all of these anomalies are due to FLL melting transitions. For example, nonlinear I-V characteristics of $NbSe_2$ (Ref. 8) and YBCO (Ref. 12) have been attributed to plastic flow or ''premelt softening'' of the FLL.

The relevant data for $NbSe_2$ or YBCO generally involve high ac field or current drives on the FL that can blur equilibrium thermal effects (e.g., melting) and nonequilibrium dynamical effects. Therefore, we have exploited the extreme sensitivity of the vibrating-reed (VR) technique[4,13] and developed a resonance-line-shape analysis that can be used to carefully differentiate the low-drive, quasilinear response from the high-drive, nonlinear response of the FL in $NbSe_2$. We have also investigated the effects of radiation damage on the FL dynamics and found strong nonlinear response near and well above the drive frequency, suggesting the onset of chaos.

When a superconducting VR is subject to applied magnetic fields parallel (''longitudinal'') or perpendicular (''transverse'') to the reed axis, diamagnetic screening currents produce a magnetic restoring force that leads to an increase $\Delta f = f - f_0$ in the resonant frequency f compared to its normal state value f_0 with decreasing temperature.[13] A single maximum in VR dissipation (proportional to inverse quality factor $1/Q$) is usually observed at or below $H_{c2}(T)$, apparently marking a boundary between mobile and immobile regimes of FL behavior, although its precise origin (e.g., FLL melting vs depinning) remains controversial.[4,14]

A vapor transport method[15] was used to grow lamellar $NbSe_2$ single crystals with residual resistance ratios (RRR) $= 30-34$ and $T_c \approx 7.2$ K. Two thin crystals (samples 1 and 2, both of thickness $t \approx 25\ \mu\text{m} \pm 15\%$ along c) were irradiated with 276 MeV Ag^{+21} ions that impacted along a direction displaced 2° from the c axis to prevent channeling (see Fig. 1). The total fluence was 8×10^{10} cm^{-2}, resulting in RRR ≈ 19 and negligible change of T_c. Standard damage analysis[16] yielded a linear energy transfer parameter of 22.3 MeV/μm and a thermalization distance (range) $R = 17.6\ \mu$m for 276 MeV Ag^{+21} ions in $NbSe_2$. Comparable irradiation

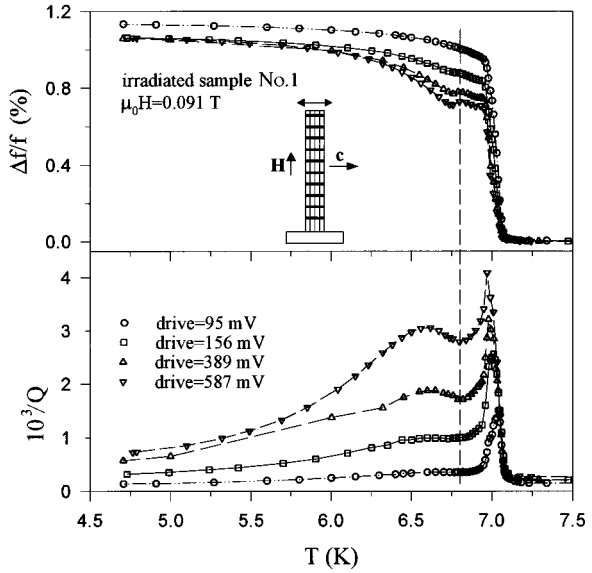

FIG. 1. Normalized frequency shift $\Delta f/f$ (top) and inverse quality factor $1/Q$ (bottom) versus temperature T for the first overtone ($f_0 = 12.1$ kHz) of a longitudinal VR at different transducer drive voltages. The inset shows a lamellar crystal mounted with the hexagonal c-axis parallel to the direction of vibration and perpendicular to the applied magnetic field **H** (longitudinal geometry). The dark lines illustrate the case of an irradiated crystal with ion tracks oriented slightly (2°) off the c direction. The vertical dashed line is a guide to the eye marking the PE.

 © 1996 The American Physical Society

conditions are known to generate (at ≈50% efficiency) columnar defects with diameters ≈60 Å in YBCO samples with $t<R$.[16] Since $R\approx t$, detailed microstructure investigations will be necessary in order to fully characterize the damage tracks in our samples.

Figure 1 shows the temperature dependence of $\Delta f/f$ and $1/Q$ of an irradiated sample taken at different drive voltages (V) in a longitudinal magnetic field $\mu_0 H=91$ mT. A narrow peak in dissipation near $T_1=7.0$ K is prominent at all drives, identifying it with a narrow, frequency-independent dissipation peak found in other measurements.[4–6] In contrast, the relative amplitude of a second, broad peak at $T_2=6.6$ K rapidly disappears for the lower drive levels, remarkably similar to the behavior of a broad anomaly found in YBCO at $T\approx 80$ K.[10] The minimum in the dissipation between T_1 and T_2 corresponds to a weak maximum in the resonant frequency. Another very small maximum in frequency can be detected at a temperature just below T_1 which also marks a tiny shoulder in $1/Q$ (see Fig. 1 for $V=389$ mV), corresponding to a small peak in $1/Q$ in nonirradiated samples where it is attributed to a PE.[4–8] Figure 1 shows that it is suppressed by radiation damage, as is the PE.[5]

It has been suggested that broad, lower temperature anomalies in the VR dissipation of high-T_c materials are not due to thermal depinning, but may be due to a phase transition of the FLL,[9] the *thermal* production of dislocations,[10] or "premelt softening" of the FLL.[11] However, the strong amplitude dependence of the T_2 anomaly in our $NbSe_2$ data and the detailed VR line-shape analysis introduced below strongly argue against interpreting such features as signatures of strictly equilibrium thermal processes.

Figure 2(a) shows two resonance curves [VR amplitude $A(f)$ versus f] taken at different transducer drives for a nonirradiated sample cooled in a longitudinal field of 1.04 T at 5.10 K. At low drives ($V<30$ mV), the resonance-line shape is Lorentzian, but for $V\gtrsim 100$ mV, the line shape becomes non-Lorentzian and "tilts" towards the low-frequency side, resembling the nonlinear response of a soft spring.[17] Figure 2(b) shows that there exists a threshold value for the VR drive $V_T\approx 120$ mV, below which the dissipation from the FL is only weakly drive dependent, but above which the dissipation rapidly increases with drive. This reinforces our suggestions that the broad peak in $1/Q$ at T_2 and the marked reduction of $\Delta f/f$ with increasing drive shown in Fig. 1 for the irradiated sample are due to a *dynamical* softening of the FLL, and not purely a thermal equilibrium process.

The resonance-line shape of irradiated samples is also Lorentzian at very low drives. However, remarkable splittings of the resonance curves occur at high drives (>200 mV) in the superconducting state only, as shown in Fig. 3. The data are acquired for the first overtone ($f_0=12.1$ kHz) of sample 1 in consecutive field-cooled cycles from $T=8.00-6.00$ K under zero drive. It is interesting that the sharp reductions in the resonance amplitude occur at approximately drive-independent frequencies separated by intervals that are multiples of a small frequency $\Delta\approx 63$ Hz. The resonance curves of the fundamental mode of vibration ($f_0=2.28$ kHz) also exhibit sharp amplitude dips with $\Delta\approx 43$ Hz under the same field and temperature conditions. The frequencies of the dips are insensitive to percent changes in temperature or the applied magnetic field. Such behavior

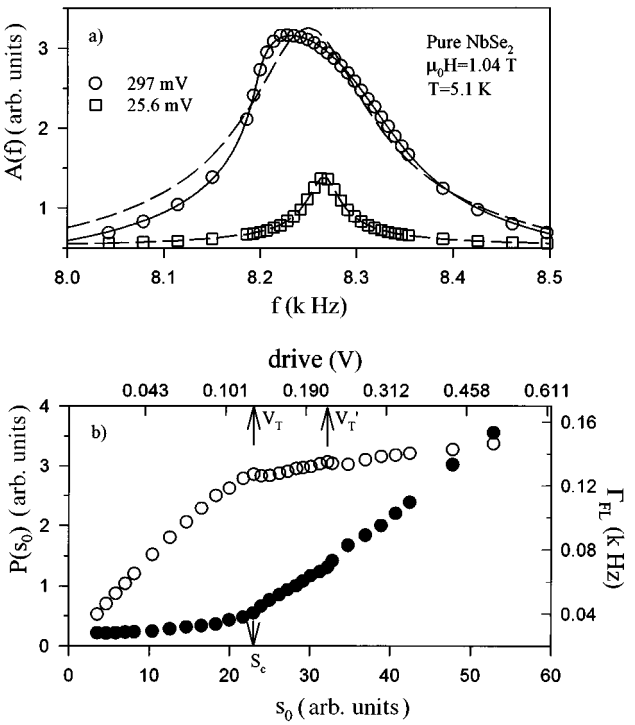

FIG. 2. (a) Resonance amplitude $A(f)$ vs drive frequency f for a longitudinal VR at two drive levels. The dashed line is a Lorentzian fit, and the solid line a fit by Eq. (3) with a nonlinear FL restoring force. (b) Maximum FL restoring force $P(s_0)$ (open symbols) and FL dissipation Γ_{FL} (solid symbols) versus FL displacement s_0. Transducer drives corresponding to s_0 values are shown on the top legend (note the nonlinear scale). V_T and s_c are a threshold drive and critical FL displacement, respectively, which mark a yield point of the FLL. V_T' is a possible second drive threshold marking the end of a transition regime (see text).

strongly suggests a self-organized pattern of dynamic response of the FL upon cooling into the mixed state. On the other hand, zero-field-cooled (ZFC) runs revealed amplitude dips at quite low drives (≈0.1 V) with unusually high background noise, which probably reflects the increased FL disorder and surface vortex density gradients incurred in ZFC conditions.

Similar results were obtained after remounting sample 1 (increasing the fundamental mode frequency by a factor of 2.8), and by performing additional measurements on irradiated sample 2. In contrast, the data for a nonirradiated sample from the same batch did not display a split line shape at any drive level. Preliminary data for damaged samples in the transverse configuration were similar to those of the nonirradiated crystal. Therefore, the results strongly suggest that anisotropic FL pinning by linear damage tracks is responsible for the split resonance curves.

The data in Fig. 3 show that peaks in the VR response repeatedly bifurcate and evolve into a broad band of response at very high drives, indicating that the reed is approaching a chaotic behavior. Therefore, we have studied the time dependence of the unfiltered reed-vibration amplitude $A(t)$ using a fast digitizing oscilloscope to search for nonlinear response over a frequency range of 0–15 MHz. Figure 4 shows the power spectra for sample 2 in three different states. The normal state response is very clean with a Lorentzian peak centered near the VR fundamental mode at f_0

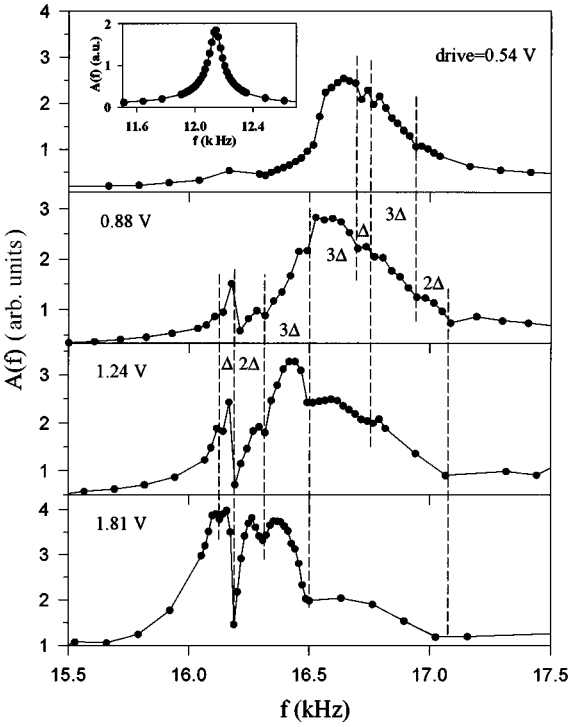

FIG. 3. Resonance amplitude $A(f)$ vs frequency f for irradiated sample 1 at high drives in a longitudinal magnetic field of 0.646 T at $T=6.00$ K. The vertical dashed lines show the invariance of amplitude dip frequencies with their characteristic separations. The solid lines are guides to the eye. Inset: a normal state curve ($T=8.00$ K) at 1.81 V drive in the same field.

$=12.1$ kHz. The low-drive (0.3 V) data in the superconducting state do not show any peak in the entire spectrum, indicating that the VR resonance signal is buried in the background noise. The high-drive (5.58 V) data in the superconducting state exhibit a shifted resonance peak at $f=14.11$ kHz, but its amplitude is heavily damped, in agreement with Fig. 3. More interesting, however, is the appearance of groups of high-amplitude peaks near 225 kHz, and

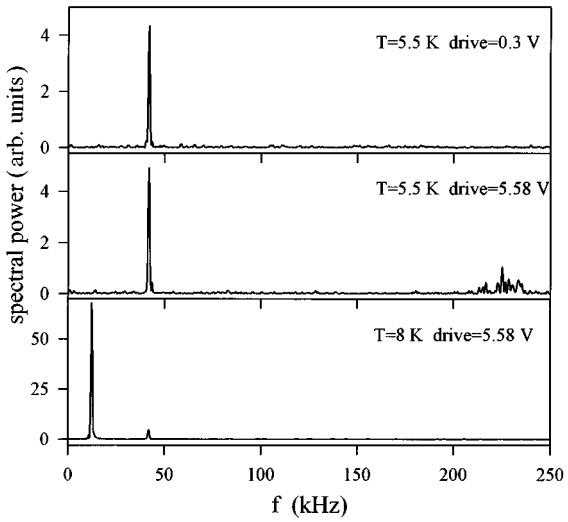

FIG. 4. Power spectra of irradiated sample 2 in a longitudinal magnetic field of 0.852 T at $T=8.00$ K (normal state) and $T=5.5$ K (superconducting state). The peak at 42 kHz is spurious since it is present in all the data, including those at zero drive.

(not shown) 4.5 and 9 MHz. These peaks are absent both in low-drive superconducting state data and in all normal state data.

A power spectrum analysis of the high-drive data is in progress. However, we have developed a mechanical oscillator analog to analyze the VR resonance curves at low-to-moderate drives. The FL are assumed to be straight and move collectively. We define $\mathbf{u}$ to be the displacement of the free end of the VR from its equilibrium position, and $\mathbf{s}$ the displacement of the FL relative to the moving VR. The FL are subject to three major forces: a damping force $-\gamma\mathbf{s}'=-\gamma\, d\mathbf{s}/dt$, a restoring force $\mathbf{P}(\mathbf{s})$, and a Lorentz force $\mathbf{J}\times\mathbf{B}$ due to the screening supercurrent $\mathbf{J}$. Since $\mathbf{J}$ is proportional to the small ac magnetic field $h\approx H[(u+s)/1]$ viewed in the moving VR frame, the Lorentz force $\approx-\alpha_1(\mathbf{u}+\mathbf{s})$, with $\alpha_1\propto H^2$ (a small demagnetizing effect is ignored in the extreme type-II limit). We expect steady state solutions of the form $u(t)=A\cos(\omega t)$ and $s(t)=s_0\cos(\omega t+\psi)$. Since our drive frequency $\omega=2\pi f\ll\omega_p$, the "pinning frequency" of free FL vibration about a pinning center, the acceleration term of the FL$\approx\mathbf{s}''$ and the inertial forces due to the noninertial VR frame can be neglected. The equation of motion for the FL reduces to

$$\mathbf{P}(\mathbf{s})-\alpha_1(\mathbf{u}+\mathbf{s})-\gamma\mathbf{s}'=0. \tag{1}$$

The equation of motion for the angular displacement $\theta=u/l$ of the VR is $\tau=I\theta''$, where I is the moment of inertia of the VR. There are five forces contributing to the torque τ on the VR: a linear mechanical restoring force $-\omega_0^2\mathbf{u}$ ($\omega_0=2\pi f_0$, the frequency of free vibrations of the VR), a damping force $-\xi\mathbf{u}'$, the transducer drive force $\sim\mathbf{F}\cos(\omega t+\phi)$, and the reaction to the Lorentz force on the FL, $-\mathbf{P}(\mathbf{s})+\gamma\mathbf{s}'$. This yields an equation of motion for $\mathbf{u}(t)$,

$$\mathbf{u}''=-\omega_0^2\mathbf{u}-\xi\mathbf{u}'-\rho^{-1}\alpha_1(\mathbf{u}+\mathbf{s})+\mathbf{F}\cos(\omega t+\phi), \tag{2}$$

where ρ is the mass density of the VR.

If the FL restoring force $\mathbf{P}(\mathbf{s})$ is known, Eqs. (1) and (2) can be solved for $\mathbf{u}(t)$ and $\mathbf{s}(t)$. For small vibrations, we assume $\mathbf{P}(\mathbf{s})\approx-\alpha\mathbf{s}$. The lowest order solutions (in the strong pinning limit $\alpha_1\ll\alpha$) are $s_0\approx-\alpha_1 A_0/\alpha$ (minus sign reflects $\psi\approx\pi$), and

$$A^2=\frac{F^2}{[\omega^2-\omega_r^2]^2+\omega^2[\xi+\gamma\alpha_1^2/(\rho\alpha^2)]^2}, \tag{3}$$

where $\omega_r^2\approx\omega_0^2+(\alpha_1/\rho)(1-\alpha_1/\alpha)$ is the VR resonant frequency in an applied magnetic field.[13] Note that the damped motion of the FL increases the reed dissipation by $\Gamma_{\rm FL}=\gamma\alpha_1^2/(\rho\alpha^2)$. Although the Lorentzian form of Eq. (3) describes the line shape of the resonance curves very well at very low drives, it does not yield good fits at high drives, reflecting the failure of a linear FL restoring force to describe the response at these drives. Alternatively, we obtained excellent fits [see Fig. 2(a)] by replacing α with a time-independent form $\alpha_{\rm eff}=\alpha_0\exp\{-A^2/u_p^2\}$ for a fixed value of transducer drive, where u_p is a scaling length related to the effective range of the FL pinning force.[18] One value of α_0 obtained from a Lorentzian fit to the lowest-drive data set was used for all drives at a given field, and values of ξ were

fixed at those obtained from fitting zero-field data at the same drive (four parameters were freely varied in the fitting procedure).

The fits yield the maximum FL restoring force $P_0 \equiv P(s_0) = \alpha_{\text{eff}} s_0$ as a function of s_0. Results for a nonirradiated sample are shown in Fig. 2(b), which clearly reveals the existence of a critical FL displacement s_c that corresponds to a threshold transducer drive $V_T \approx 120$ mV, below which P_0 is quasilinear in s_0, and above which P_0 is drastically reduced below the linear trend. Note that P_0 exhibits a small drop near V_T, recalling the stress-strain curves of many ionic crystals, where it is termed "discontinuous yield,"[19] and attributed to a sharp increase in the density of mobile dislocations at the onset of large-scale plastic deformation. A second threshold may exist near a higher drive $V_T' \approx 210$ mV (defining a "transition regime," $V_T < V < V_T'$), beyond which we find that the FL dissipation is markedly linear in VR drive voltage with reduced scatter in the data. Although these effects are small, they were consistently observed in all our data sets, and may well correspond to the three regimes of FL response inferred from I-V measurements.[8]

The irradiated samples do not exhibit a sharp threshold V_T; rather, P_0 smoothly bends over at moderate drives, and continues to rise at higher drives. The strong pinning provided by the damage tracks must inhibit the motion of correlated FL domains and allow larger stresses to build up in the FLL with increasing drive, which is probably related to the onset of the amplitude dips observed at high drives in Fig. 3. The simple topology of the VR and the small magnitude of $\Delta \approx 40-60$ Hz suggest that structures in the resonant response are principally dependent on small changes of the macroscopic length scales that govern the dynamical restoring forces and damping near the free end of the reed where the vibration amplitude is maximal. When stress builds to a threshold value, domains within the FLL may begin to break away or decorrelate from larger bodies of FLL near the tip of the reed, causing an abrupt reduction in the restoring force and an increase in dissipation as screening currents reroute away from the tip. A crude estimate of such "dynamic shortening" of the VR may be made by noting $\omega_r^2 \approx \omega_0^2 + (\alpha_1/\rho)(1-\alpha_1/\alpha) \equiv \omega_0^2 + \omega_\alpha^2$, where ω_α^2 is the shift of the squared VR frequency due to the pinning of FL.[13] If finite drive "depins" FL over a length δl near the free end of the VR, the restoring force decreases and the squared frequency is reduced by $\delta(\omega_r^2) = 2\omega_r \delta\omega_r = 2\omega_1 \Delta \approx \omega_\alpha^2(\delta l/1)$, where Δ is the characteristic separation between amplitude dips. Using values from Fig. 3 with $l \approx 3$ mm, we get $\delta l \approx 50$ μm, which may be interpreted as an upper limit for the correlation length of the "unpinned" FLL along the VR axis.

In summary, the flux-line restoring force in $NbSe_2$ exhibits a quasilinear elastic regime and a nonlinear, highly dissipative regime separated by a yield point that marks the onset of plastic deformation of the flux-line lattice, followed by a "noisy" transition regime and a second threshold marking the onset of a third regime corresponding to "elastic flow" proposed by Bhattacharya and Higgins.[8] Depending on field/cooling history and drive, the resonance curves of irradiated samples bifurcate, exhibiting strong dissipative anomalies separated by characteristic frequency intervals that may mark the onset of chaos. Strong nonlinear response also develops at frequencies much higher than the drive frequency at very high drives relevant for many practical applications of superconductors. We postulate that the characteristic amplitude dips occur at frequencies for which no single current pattern is particularly stable and self-organized reconfigurations of the screening currents take place (possibly accompanied by FL avalanches) to minimize overall VR dissipation as the drive frequency is tuned through the broadened frequency response. We conclude that nonlinear, nonequilibrium FL response must be considered in interpreting mixed state dissipative processes and associated evidence for vortex phase transitions.

Recently, Yaron *et al.*[20] have published small-angle neutron-scattering data for undamaged $NbSe_2$ that corroborate many of the ideas presented here; in particular they identify three regimes of elastic/plastic behavior of the FLL.

We would like to thank G. Canright, J. W. Brill, and G. W. Lehman for stimulating discussions. Research at the University of Kentucky was supported by NSF Grant No. EHR-91-08764, and at Brookhaven National Lab by U.S. DOE Office of Basic Energy Sciences, Division of Materials Science, Contract No. DE-AC02-76CH00016.

*Present address: Dept. of Physics, I.I.T. Kanpur, Kanpur 208016, India.

[1] L. Civale *et al.*, Phys. Rev. Lett. **67**, 648 (1991); M. Konczykowski *et al.*, Phys. Rev. B **44**, 7167 (1991).
[2] G. Blätter *et al.*, Rev. Mod. Phys. **66**, 1125 (1994).
[3] W. Jiang *et al.*, Phys. Rev. Lett. **74**, 1438 (1995); D. Farrell *et al.* Phys. Rev. B **51**, 9148 (1995).
[4] Z. Xu *et al.*, Physica C **202**, 256 (1992); Z. Xu, H. Drulis, L. E. De Long, and J. W. Brill, J. Phys. (Paris) Colloq. **3**, C2-27 (1993).
[5] M. Chung *et al.*, Phys. Rev. B **50**, 1329 (1994).
[6] G. D'Anna *et al.*, Physica C **218**, 238 (1993).
[7] P. Koorevaar *et al.*, Phys. Rev. B **42**, 1004 (1990); T. W. Jing and N. P. Ong, *ibid.* **42**, 10 781 (1990).
[8] S. Bhattacharaya and M. J. Higgins, Phys. Rev. Lett. **70**, 2617 (1993).
[9] Y. Kopelevich, A. Gupta, and P. Esquinazi, Phys. Rev. Lett. **70**, 666 (1993).
[10] M. Ziese *et al.*, Phys. Rev. B **50**, 9491 (1994).
[11] X. Ling and J. I. Budnick, in *Magnetic Susceptibility of Superconductors and Other Spin Systems*, edited by R. A. Hein *et al.* (Plenum, New York, 1991), p. 377; G. D'Anna *et al.*, Europhys. Lett. **25**, 225 (1994).
[12] W. K. Kwok *et al.*, Phys. Rev. Lett. **73**, 2614 (1994).
[13] P. Esquinazi, J. Low Temp. Phys. **85**, 139 (1991).
[14] E. H. Brandt, J. Alloys Compounds **181**, 339 (1992).
[15] R. Kershaw, M. Vlasse, and A. Wold, Inorg. Chem. **6**, 1599 (1967).
[16] Y. Zhu *et al.*, Phys. Rev. B **48**, 6436 (1993), and references therein.
[17] J. M. T. Thompson and H. B. Stewart, *Nonlinear Dynamics and Chaos* (Wiley, New York, 1986).
[18] A. M. Campbell, J. Phys. C **4**, 3186 (1971).
[19] M. T. Sprackling, *The Plastic Deformation of Simple Ionic Crystals* (Academic, New York, 1976).
[20] U. Yaron *et al.*, Nature (London) **376**, 753 (1995).